doi:10.1093/brain/awv203 BRAIN 2015: 138; 2571–2583 | 2571

BRAIN
A JOURNAL OF NEUROLOGY

Permeability of the blood–brain barrier predicts conversion from optic neuritis to multiple sclerosis

Stig P. Cramer,[1] Signe Modvig,[2] Helle J. Simonsen,[1] Jette L. Frederiksen[2,3] and Henrik B. W. Larsson[1,3]

See Naismith and Cross (doi:10.1093/brain/awv196) for a scientific commentary on this article.

Optic neuritis is an acute inflammatory condition that is highly associated with multiple sclerosis. Currently, the best predictor of future development of multiple sclerosis is the number of T_2 lesions visualized by magnetic resonance imaging. Previous research has found abnormalities in the permeability of the blood–brain barrier in normal-appearing white matter of patients with multiple sclerosis and here, for the first time, we present a study on the capability of blood–brain barrier permeability in predicting conversion from optic neuritis to multiple sclerosis and a direct comparison with cerebrospinal fluid markers of inflammation, cellular trafficking and blood–brain barrier breakdown. To this end, we applied dynamic contrast-enhanced magnetic resonance imaging at 3 T to measure blood–brain barrier permeability in 39 patients with monosymptomatic optic neuritis, all referred for imaging as part of the diagnostic work-up at time of diagnosis. Eighteen healthy controls were included for comparison. Patients had magnetic resonance imaging and lumbar puncture performed within 4 weeks of onset of optic neuritis. Information on multiple sclerosis conversion was acquired from hospital records 2 years after optic neuritis onset. Logistic regression analysis showed that baseline permeability in normal-appearing white matter significantly improved prediction of multiple sclerosis conversion (according to the 2010 revised McDonald diagnostic criteria) within 2 years compared to T_2 lesion count alone. There was no correlation between permeability and T_2 lesion count. An increase in permeability in normal-appearing white matter of 0.1 ml/100 g/min increased the risk of multiple sclerosis 8.5 times whereas having more than nine T_2 lesions increased the risk 52.6 times. Receiver operating characteristic curve analysis of permeability in normal-appearing white matter gave a cut-off of 0.13 ml/100 g/min, which predicted conversion to multiple sclerosis with a sensitivity of 88% and specificity of 72%. We found a significant correlation between permeability and the leucocyte count in cerebrospinal fluid as well as levels of CXCL10 and MMP9 in the cerebrospinal fluid. These findings suggest that blood–brain barrier permeability, as measured by magnetic resonance imaging, may provide novel pathological information as a marker of neuroinflammation related to multiple sclerosis, to some extent reflecting cellular permeability of the blood–brain barrier, whereas T_2 lesion count may more reflect the length of the subclinical pre-relapse phase.

1 Functional Imaging Unit, Department of Clinical Physiology, Nuclear Medicine and PET, Rigshospitalet, Nordre Ringvej 57, 2600 Glostrup, Denmark
2 Department of Neurology, Rigshospitalet, Nordre Ringvej 57, 2600 Glostrup, Denmark
3 Institute of Clinical Medicine, The Faculty of Health Science, University of Copenhagen, Blegdamsvej 3B, 2200 København N, Denmark

Correspondence to: Stig P. Cramer, MD. PhD
Functional Imaging Unit,

Received January 19, 2015. Revised May 28, 2015. Accepted June 9, 2015. Advance Access publication July 17, 2015

Department of Clinical Physiology, Nuclear Medicine and PET, Rigshospitalet, Nordre Ringvej 57, 2600 Glostrup, Denmark,
E-mail: stig.praestekjaer.cramer@regionh.dk

Keywords: blood–brain barrier; optic neuritis; multiple sclerosis; DCE-MRI; perfusion MRI

Abbreviations: BBB = blood–brain barrier; DCE-MRI= dynamic contrast-enhanced MRI; IgG = immunoglobulin G

Introduction

Optic neuritis is an acute multi-aetiological inflammatory condition affecting the optic nerve causing retro-orbital pain and visual loss. Optic neuritis is highly associated with multiple sclerosis, and 50% of cases develop multiple sclerosis after 15 years (Optic Neuritis Study Group, 2008). MRI currently provides one of the best risk stratification markers for later conversion to multiple sclerosis, as 72% of cases having more than one multiple sclerosis-specific white matter lesion at baseline subsequently develop multiple sclerosis, as opposed to 25% with no multiple sclerosis-specific lesions at baseline (Optic Neuritis Study Group, 2008). We have recently published data showing that patients with multiple sclerosis have a higher permeability of the blood–brain barrier (BBB) in the normal-appearing white matter when compared to healthy control subjects, and furthermore, when patients had recently experienced a clinical relapse the permeability increased significantly.

The optic nerve is considered a part of the CNS as it is derived from an out-pouching of the diencephalon during embryonic development. As a consequence of this it shares many histological characteristics with the diencephalon, i.e. myelination is produced by oligodendrocytes, it is ensheathed by three meningeal layers and has a BBB, etc. During acute optic neuritis, a common MRI finding is contrast enhancement of the optic nerve, indicative of BBB breakdown. However, little is known of the behaviour of the BBB in the normal-appearing tissue of the telencephalon during the acute stages of optic neuritis. Therefore, we wanted to investigate whether patients with optic neuritis also have changes of the BBB permeability in normal-appearing white matter normal as we have seen in patients with multiple sclerosis (Cramer *et al.*, 2014). In addition, we wanted to investigate if a leakier BBB in these patients could be related to other measures of neuroinflammation, and whether the degree of leakiness could be related to the likelihood of developing multiple sclerosis within a period of 2 years. The BBB permeability was investigated by use of dynamic contrast-enhanced T_1-weighted MRI (DCE-MRI) (Larsson *et al.*, 2009).

Materials and methods

Optic neuritis patients and healthy volunteers

Thirty-nine patients with acute optic neuritis were enrolled prospectively in the study. From June 2011 to December 2012 134 patients were referred by ophthalmologists to the Clinic of Optic Neuritis, Glostrup Hospital with suspected optic neuritis. Diagnostic criteria were as previously described (Modvig *et al.*, 2013). In short, inclusion criteria were: a diagnosis of optic neuritis, time from onset of visual symptoms to MRI and lumbar puncture $\leqslant$28 days, age between 18 and 59 years and no prior symptoms of demyelinating disease. Thirty-nine (60%) of 65 eligible patients participated in the study (Supplementary Fig. 1).

Multiple sclerosis diagnosis and risk factors

A diagnosis of multiple sclerosis was made by experienced multiple sclerosis clinicians using the revised 2010 McDonald criteria (Polman *et al.*, 2011). As MRI risk factors of multiple sclerosis we chose T_2 lesion count, divided into three categories (0–1 lesion, 2–8 lesions and $>$9 lesions) based on previous results showing low and high risk of multiple sclerosis in the 0–1 lesion group and $>$9 lesions groups, respectively (Barkhof *et al.*, 1997; Tintoré *et al.*, 2000; Optic Neuritis Study Group, 2008). Information on multiple sclerosis development was acquired from hospital records 2 years after optic neuritis onset.

Healthy controls

Eighteen healthy controls were enrolled on the basis of age and gender, 12 of these were part of a previously described group (Modvig *et al.*, 2013) who underwent lumbar puncture. None had a history of autoimmune, neurological, or chronic illness, nor any prior symptoms or family history of demyelinating disease. All underwent a thorough clinical and neurological examination. Multiple sclerosis patients and healthy controls had MRI scans performed in an interleaved fashion to minimize the impact of slight scanner hardware differences (i.e. scanner drift) over time on the results.

CSF sampling and biomarker analysis

All 39 patients gave consent for usage of routine lumbar puncture values [CSF leucocyte count, immunoglobulin G (IgG) index and oligoclonal bands], whereas 34 of 39 patients gave consent for acquisition of additional study biomarkers from CSF. Twelve of 18 healthy controls gave consent for lumbar puncture and acquisition of study biomarkers. Routine analysis included CSF leucocyte and erythrocyte counts, measurement of CSF protein and glucose levels, IgG index and albumin quotient and test for oligoclonal bands by isoelectric focusing and immunoblotting. CSF (12 ml) was collected in an ice bath and immediately centrifuged at 400*g* at 4°C for 10 min, and the cell-free supernatant was frozen and stored in 0.5 ml aliquots at −80°C until analysis. Levels of the biomarkers C-X-C motif chemokine 10 (CLCX10), C-X-C

motif chemokine 13 (CLCX13) and matrix metalloproteinase 9 (MMP9) were analysed by enzyme-linked immunosorbent assays (ELISA) using commercially available kits as previously described (Modvig *et al.*, 2013).

Imaging

Magnetic resonance sequences and regions of interest

MRI was performed on a 3 T MRI unit (Philips Achieva) using a 32-element phased-array head coil. We used an axial T_2-weighted MRI sequence [five slices, echo time = 100 ms, repetition time = 3000 ms, acquired voxel-size 0.57/0.76/8 mm^3 (interpolated to 0.45/0.45/8 mm^3), field of view = 230 × 119 mm^2] with same orientation and slice thickness (8 mm) as our DCE-MRI sequence, in order to manually draw regions of interest in the periventricular normal-appearing white matter, and in the normal-appearing thalamic grey matter in both hemispheres, avoiding inclusion of or proximity to any multiple sclerosis lesions, as previously described in detail (Cramer *et al.*, 2014). Examples of region of interest placement can be seen in Figs 1–3. T_2 lesions were defined as a T_2 hyperintensity >3 mm in size with a typical anatomical location for multiple sclerosis, i.e. periventricular, juxtacortical or infratentorial. In addition T_2 lesions >3 mm in size in subcortical and deep white matter were also included in total T_2 lesion count. This procedure was performed by an experienced neuroradiologist using an axial T_2 fluid attenuation inversion recovery (FLAIR) sequence [35 slices, echo time = 125 ms, repetition time = 11 000 ms, acquired voxel-size 0.65/0.99/3.5 mm^3 (interpolated to 0.45/0.45/3.5 mm^3), field-of-view = 230 × 119 mm^2, slice thickness of 3.5 mm].

Dynamic contrast enhanced MRI

DCE-MRI used a T_1-weighted saturation-recovery gradient-echo sequence with flip angle 30°, repetition time = 3.9 ms, echo time = 1.9 ms, centric phase ordering, parallel imaging factor 2, acquired matrix 96 × 61, acquired voxel-size 2.40/2.98/8 mm^3 (interpolated to 0.90/0.89/8 mm^3), field of view 230 × 182 mm^2, five slices, slice thickness 8 mm. Data for an initial measurement of relaxation time (T_1) and equilibrium magnetization (M_0) were generated using a series of saturation time delays from 120 ms to 10 s, covering the same slices as imaged during the bolus passage. The dynamic sequence used a saturation time delay of 120 ms, giving a time resolution of 1.25 s, and 750 time points, corresponding to a total sampling duration 15.7 min. More details can be found in Cramer *et al.* (2014).

Permeability estimation

The DCE-MRI data were analysed with a semi-automatic procedure (Larsson *et al.*, 2008) using in-house MatLab-based software. The DCE-MRI time series was converted to units of contrast agent concentration using T_1 and M_0 (Cramer *et al.*, 2014). The input function was corrected for partial volume by normalizing to a phase-derived venous outflow function, free of any partial volume effects (van Osch *et al.*, 2001), sampled in the sagittal sinus (Hansen *et al.*, 2009). Tissue concentration-time curves were evaluated using a combination of model free deconvolution and a two-compartment model, after which the median value was taken from each region of interest, as described in previous work (Larsson *et al.*, 2009). Permeability values are reported as K_i in the unit of ml/100 g/min assuming brain tissue density of 1 g/ml [$K_i = K^{trans}/(1 - Hct)$].

Statistics

We used Mann-Whitney U-tests and Spearman rank correlations due to small sample size and a *P*-value lower than 0.05 to allow us to reject the null hypothesis. Forward stepwise logistic regression with multiple sclerosis at 2 years as outcome was used to estimate the relative risk increase for the different risk factors. Receiver operating characteristic (ROC) curves were used to estimate the ability of a risk factor to predict conversion to multiple sclerosis and establish a cut-off value providing the best combined sensitivity and specificity.

Ethics

This study was approved by the Ethics Committee of Copenhagen County according to the standards of The National Committee on Health Research Ethics, protocol number H-D-2008-002 (MRI protocol) and H1-2011-019 (biomarker protocol). All experiments were conducted in accordance with the Declaration of Helsinki of 1975 and all subjects gave written informed consent.

Results

Baseline characteristics of patients with optic neuritis and healthy controls are shown in Table 1. There were no significant differences in age and gender between patients and healthy controls. Seventeen patients of 39 (44%) were diagnosed with multiple sclerosis during the observation period of 2 years and the frequency of clinical visits and MRI scans in this group was not influenced by the study protocol. Thirteen of these 17 multiple sclerosis converters (94%) were started on first line disease-modifying treatment within 2–6 weeks after baseline visit. Four of these after a diagnosis of multiple sclerosis was made on the first scan, and the remaining as preventative treatment due to perceived high risk of future multiple sclerosis development (Fig. 4). The decision of initiating first line disease-modifying treatment (Interferon beta 1a in all cases) was made by an experienced multiple sclerosis neurologist at the multiple sclerosis clinic at Glostrup Hospital and was not influenced by the study in any way. Prophylactic disease-modifying treatment was initiated in accordance with international recommendations (Clerico *et al.*, 2008) within 2–6 weeks after onset of optic neuritis. The timing of initiation of treatment and diagnosis of multiple sclerosis for the patients who converted to multiple sclerosis can be seen in Fig. 4. One patient was transferred to another healthcare centre during the observation period and was excluded from analysis related to multiple sclerosis risk. The remaining 21

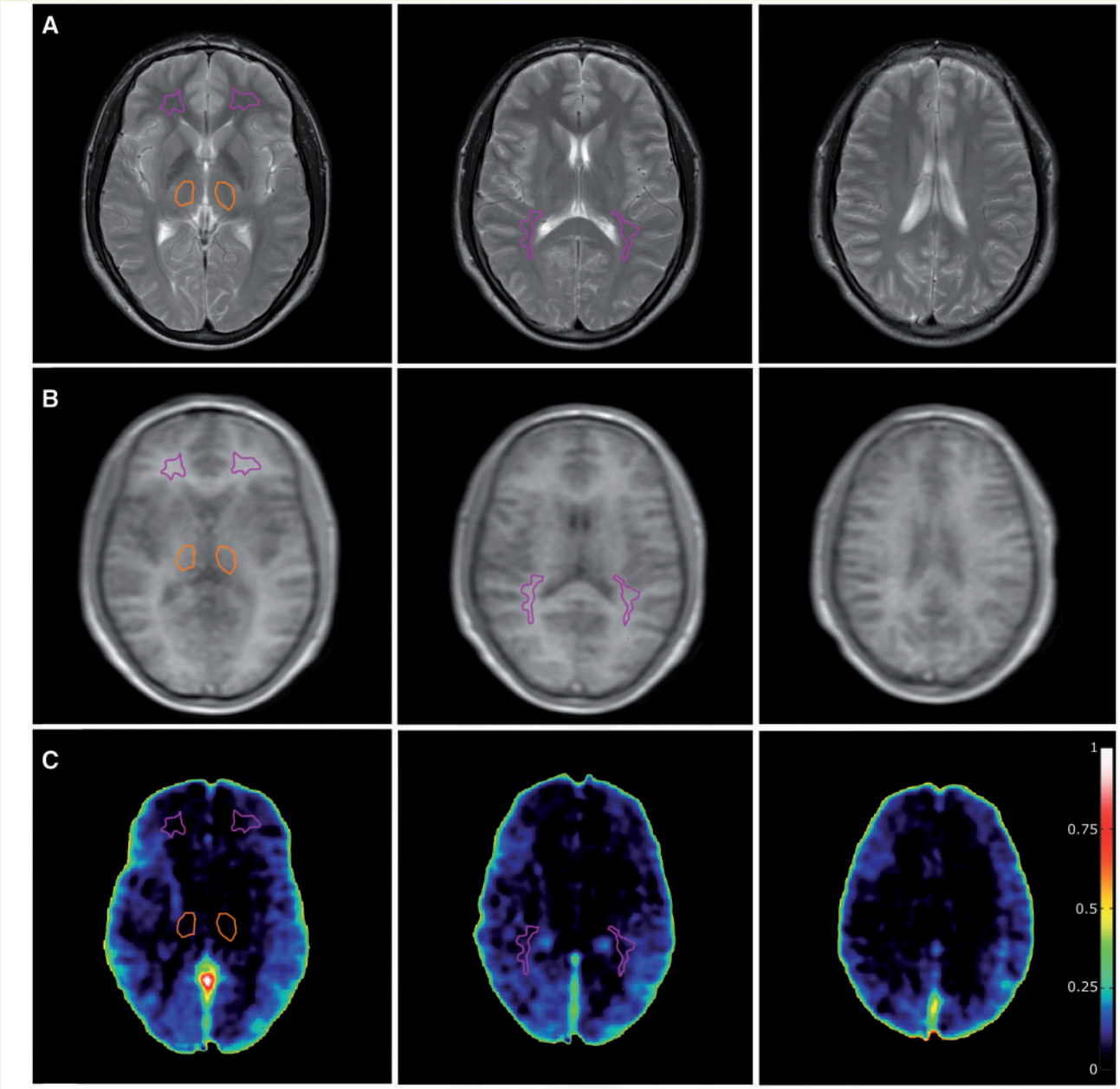

Figure 1 Healthy control subject. (**A**) T_2-weighted sequence on which region of interest placement is performed. Purple: normal-appearing white matter; orange: thalamus; red: lesions. (**B**) Corresponding DCE slices. (**C**) Voxel-wise permeability maps, measured as K_i in ml/100 g/min.

patients who were not diagnosed with multiple sclerosis during the 2-year period all had a minimum of one routine MRI at 6 months and clinical assessment at 12 months to make sure that none had new MRI lesions or relapses. Six of the 21 non-converters (29%) were started on disease-modifying treatment within 2–6 weeks after onset of optic neuritis. At 2 years after optic neuritis onset, clinical assessment was made either in person ($n = 10$) or by telephone interview ($n = 11$). Example permeability maps from one healthy control and two optic neuritis patients; one multiple sclerosis converter and one non-converter can be seen in Figs 1–3.

BBB permeability and risk of multiple sclerosis

In the whole group of optic neuritis patients we found a significantly higher BBB permeability in periventricular normal-appearing white matter compared to healthy control subjects ($P = 0.017$; Mann-Whitney U-test) (Table 1 and Supplementary Fig. 2). In deep grey matter (thalamus) the two groups had similar permeability values. In patients who developed multiple sclerosis within 2 years from optic neuritis onset ($n = 17$), we found significantly higher permeability in normal-appearing white matter ($P = 0.004$;

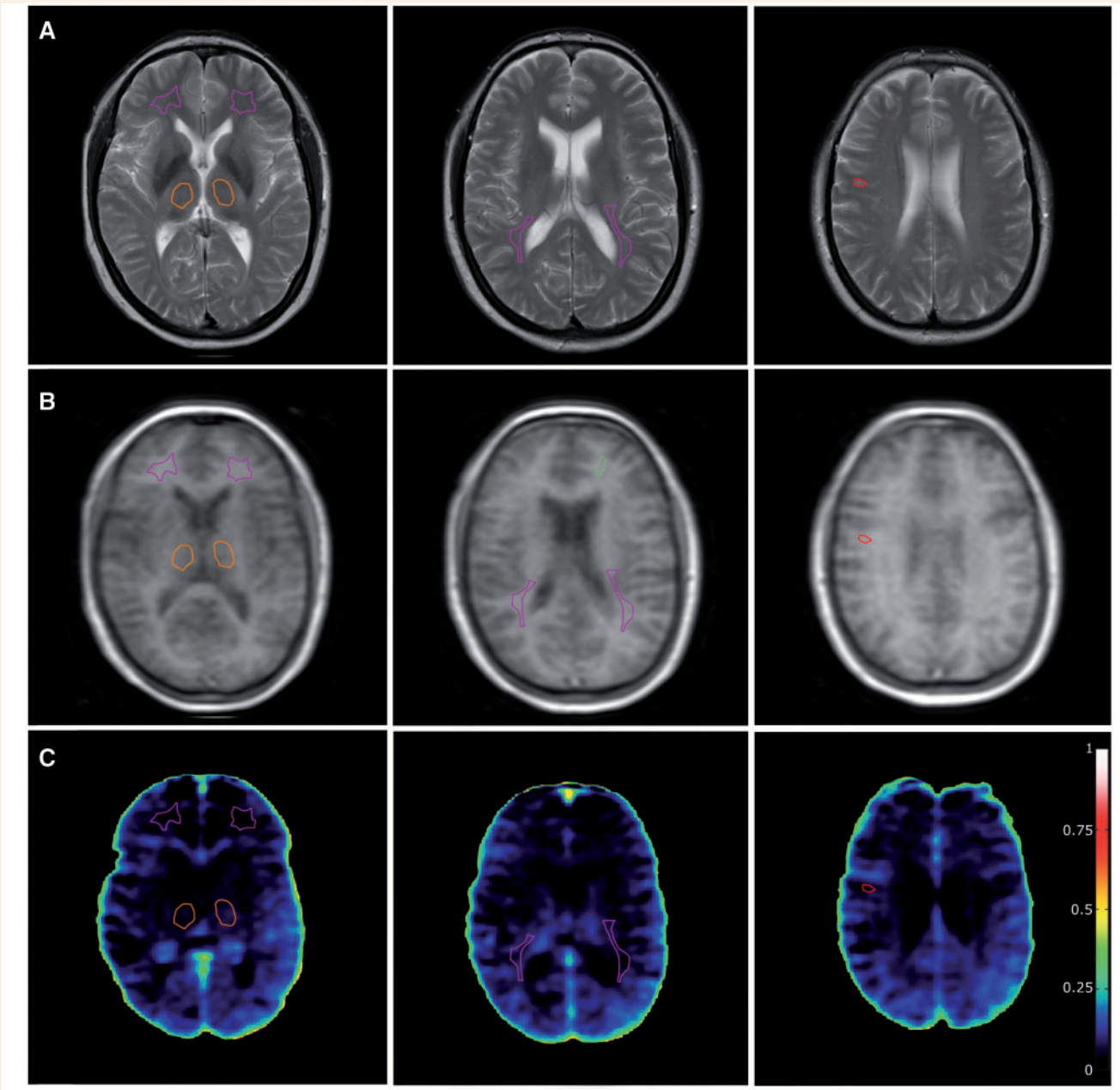

Figure 2 Patient with optic neuritis that did not convert to multiple sclerosis. (**A**) T_2-weighted sequence on which region of interest placement is performed. Purple: normal-appearing white matter; orange: thalamus; red: lesions. (**B**) Corresponding DCE-MRI slices. (**C**) Voxel-wise permeability maps, measured as K_i in ml/100 g/min.

Mann-Whitney U-test) and in the thalamus ($P = 0.003$; Mann-Whitney U-test) compared to patients who did not develop multiple sclerosis ($n = 21$). To investigate how well BBB permeability at optic neuritis onset predicted conversion to multiple sclerosis after 2 years, we performed a forward stepwise multivariate logistic regression analysis (Table 2). Having >9 T_2 lesions on baseline MRI increased the risk of multiple sclerosis 52.6 times ($P = 0.002$) as previously shown (Barkhof *et al.*, 1997; Tintoré *et al.*, 2000). An increase in permeability in normal-appearing white matter of 0.1 ml/100 g/min increased the risk 8.5 times ($P = 0.03$). Model Nagelkerke $R^2 = 0.60$, $P = 0.007$. Number of T_2 lesions alone provided a Nagelkerke $R^2 = 0.47$, but adding permeability in normal-appearing white matter significantly improved prediction of multiple sclerosis development ($P = 0.007$). To calculate the best cut-off value for permeability in normal-appearing white matter for multiple sclerosis prediction we conducted a ROC analysis, yielding an area under the curve of 0.77 [95% confidence interval (CI) 0.60–0.93], $P = 0.005$ (Table 3). A threshold of permeability in normal-appearing white matter >0.13 ml/100 g/min predicted conversion to multiple sclerosis with a sensitivity of 88% and a specificity of 72%. For comparison ROC curve specifications for

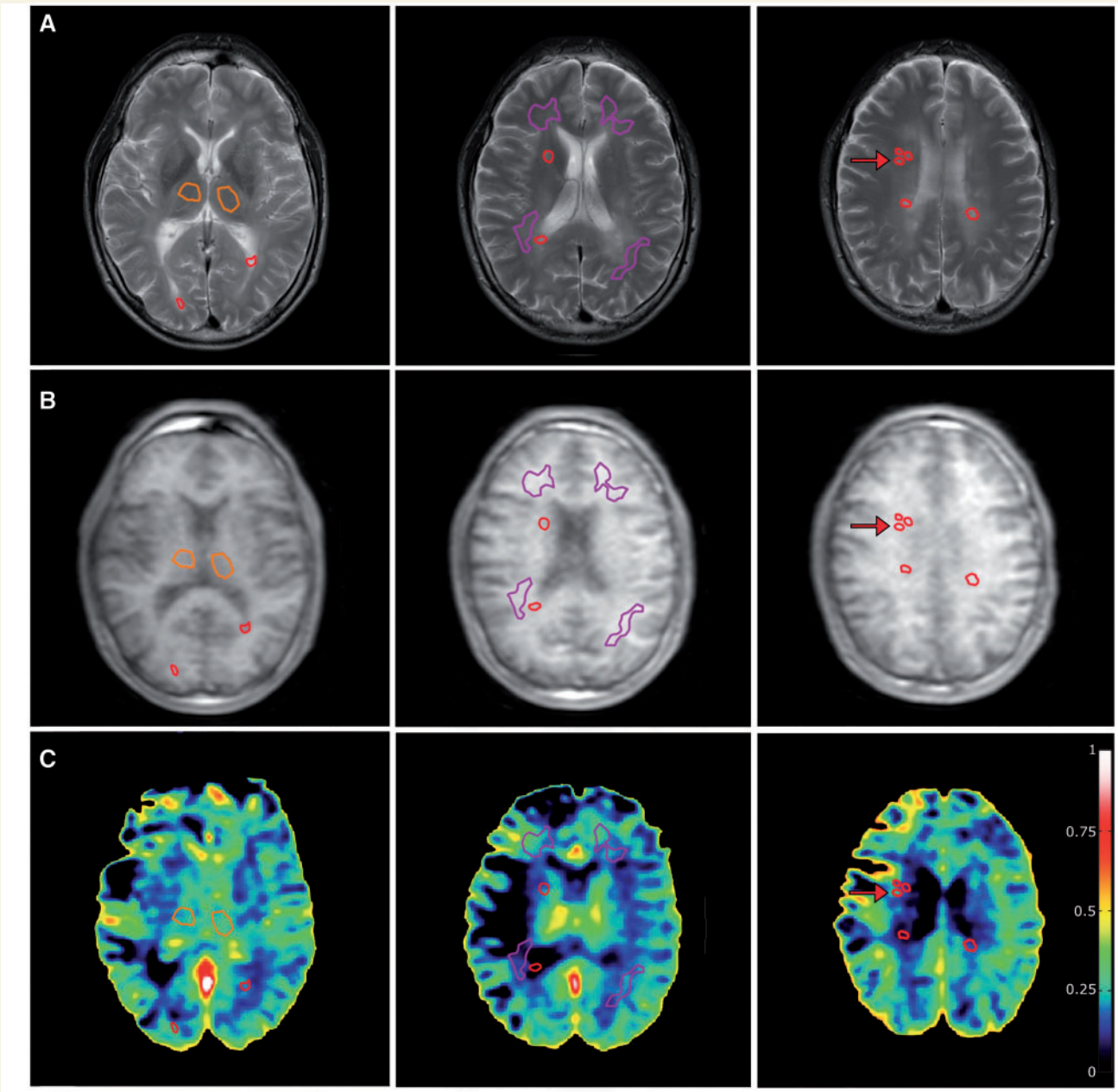

Figure 3 Optic neuritis patient with conversion to multiple sclerosis. (**A**) T_2-weighted sequence on which region of interest placement is performed. Purple: normal-appearing white matter; Orange: thalamus; Red: lesions. (**B**) Corresponding DCE slices. (**C**) Voxel-wise permeability maps, measured as K_i in ml/100 g/min. Note the higher permeability values in normal-appearing white matter, when compared to Fig. 2, which has the same scaling. A small contrast-enhancing lesion that was visible on post-contrast T_1 image (not shown) is marked by red arrows. Note that the model fit is more prone to noise-related errors when conducted on a voxel-wise basis compared to the region of interest-based approach used in the article. Also note that the high permeability values in some parts of the ventricular system are caused by the choroid plexus, where fenestrated capillaries and lack of tight junctions allow passage of contrast agent into the interstitial spaces.

other predictors of multiple sclerosis development can also be seen in Table 3. Comparing permeability in normal-appearing white matter to T_2 lesion count we found no significant difference between ROC curve areas under the curve ($P = 0.42$ and $P = 0.44$, respectively). CSF leucocytosis has previously been shown to predict conversion from clinically isolated syndrome to clinically definite multiple sclerosis (Gout *et al.*, 2011; Modvig *et al.*, 2015), but leucocyte count just fell outside significance in the logistic regression model. Permeability in normal-appearing white matter and in the thalamus were significantly correlated in the optic neuritis patients [correlation coefficient (CC) 0.62, $P = 0.00002$]. Entering permeability in thalamus (instead of normal-appearing white matter to avoid colinearity) to the logistic regression analysis showed that permeability in the thalamus together with T_2 lesion count was also a

Table 1 Clinical characteristics of optic neuritis patients and healthy controls

	ON patients; all ($n = 39$)	ON patients; MS converters ($n = 17$)	ON patients; non-converters ($n = 21$)	Healthy controls ($n = 18$)	*P*-value for difference[c]
Age (years)[a]	37 (10)	37 (10)	38 (13)	33(10)	0.16
Gender (number of females)	33 (77%)	11 (65%)	18 (86%)	12 (67%)	0.41
Haematocrit	0.43 (0.03)	0.44 (0.03)	0.42 (0.03)	0.42 (0.03)	0.14
Blood–brain barrier permeability (ml/100 g/min)					
Periventricular NAWM[a]	0.15 (0.07)	0.18 (0.08)	0.12 (0.05)	0.10 (0.05)	0.017
ROI size (voxels)	118 (53)	122 (62)	109 (49)	135 (71)	0.32
Thalamic grey matter[a]	0.12 (0.06)	0.14 (0.06)	0.09 (0.05)	0.11 (0.06)	0.74
ROI size (voxels)	113 (30)	111 (36)	117 (23)	101 (41)	0.22
Biomarkers in CSF				**($n = 12$)**	
Positive IgG index	16 (42%) ($n = 38$)[e]	8 (50%)	8 (38%)	0	–
Positive OCB	25 (64%) ($n = 39$)	14 (82%)	10 (48%)	0	–
Leucocytes (mio/l)[b]	9 (12) ($n = 38$)[e]	15 (15)	5 (5)	3 (2)	0.001
CXCL10 (pg/ml)[b]	268 (227) ($n = 34$)	364 (287)	199 (132)	128 (85.3)	0.012
CXCL13 (pg/ml)[b]	37.7 (87.9) ($n = 34$)	57.0 (125)	23.7 (40.0)	3.9[d]	0.0005
MMP9 (ng/ml)[b]	0.66 (1.24) ($n = 34$)	1.13 (1.77)	0.30 (0.24)	0.156[d]	0.001

[a]Mean and standard deviation.
[b]Median and interquartile range.
[c]Between all optic neuritis patients and healthy controls. Mann-Whitney U or chi square tests where appropriate.
[d]All healthy controls had below threshold values.
[e]Due to high erythrocyte count in CSF we excluded IgG index and leucocyte count one patient.
MS = multiple sclerosis; NAWM = normal-appearing white matter; ON = optic neuritis; OCB = oligoclonal bands; ROI = region of interest.

significant predictor of multiple sclerosis development (OR 8.3; $P = 0.035$). We found no correlation between permeability in normal-appearing white matter and the T_2 lesion count (Spearman CC = 0.13, $P = 0.44$) (Supplementary Fig. 3) or T_2 lesions load (CC = 0.25, $P = 0.19$) indicating that permeability and T_2 lesions may provide different pathophysiological information.

Correlations between BBB permeability and CSF biomarkers

The results of the correlation analysis can be seen in Table 4. For patients with optic neuritis we found a significant correlation between BBB permeability and CSF leucocyte count; Spearman correlation coefficient (CC) = 0.57; $P = 0.0002$ (Fig. 5). For CLCX10 we found a CC of 0.40 ($P = 0.02$) with BBB permeability. The MMP9 values of 13 patients were below the detection limit of the assay, for which reason we used a censored regression analysis (Tobit) to avoid improper weighting of the large number of non-detectable values. This analysis showed a significant linear trend ($P = 0.034$). We found no significant correlations between permeability in normal-appearing white matter and CLCX13 ($P = 0.24$), neither did we find any correlations between permeability in the thalamus and CSF leucocytes ($P = 0.06$), CLCX10 ($P = 0.31$), MMP9 ($P = 0.06$) or CLCX13 ($P = 0.06$). There were significant intercorrelations between the following CSF biomarkers: CSF leucocyte count, IgG index, oligoclonal bands, CLCX10, CLCX13 and MMP9, as previously shown by us and others (Sellebjerg and Sorensen, 2003; Khademi *et al.*, 2011; Modvig *et al.*, 2013).

Discussion

In this study of a prospective cohort of optic neuritis patients we found that BBB permeability measured by DCE-MRI in periventricular normal-appearing white matter and the thalamus provides prognostic information about multiple sclerosis conversion after 2 years. MRI measured permeability seems to provide supplementary information compared to existing MRI risk parameters, as it is neither correlated to T_2 lesion count nor T_2 lesion load. This indicates that the BBB permeability changes observed in this study are not simply the result of secondary myelin degradation and BBB damage due to Wallerian or retrograde degeneration. Moreover, we found that BBB permeability is correlated with CSF leucocyte count, CLCX10 and MMP9 concentrations in CSF. CXCL10 is a chemokine that attracts activated T cells through its receptor, CXCR3, and it is present at higher concentrations in the CSF of multiple sclerosis patients with active demyelinating attacks when compared to neurological controls (Sorensen *et al.*, 2001). MMP9 is secreted by lymphocytes and macrophages, facilitating their migration across glia limitans basement membranes (Leppert, 1998; Avolio *et al.*, 2003), and MMP9 has been suggested as a surrogate marker of disease activity in multiple sclerosis (Sellebjerg and Sorensen, 2003). The association between these CSF biomarkers and MRI quantification of BBB permeability seems to suggest that although the method is Gd-DTPA based, it may to

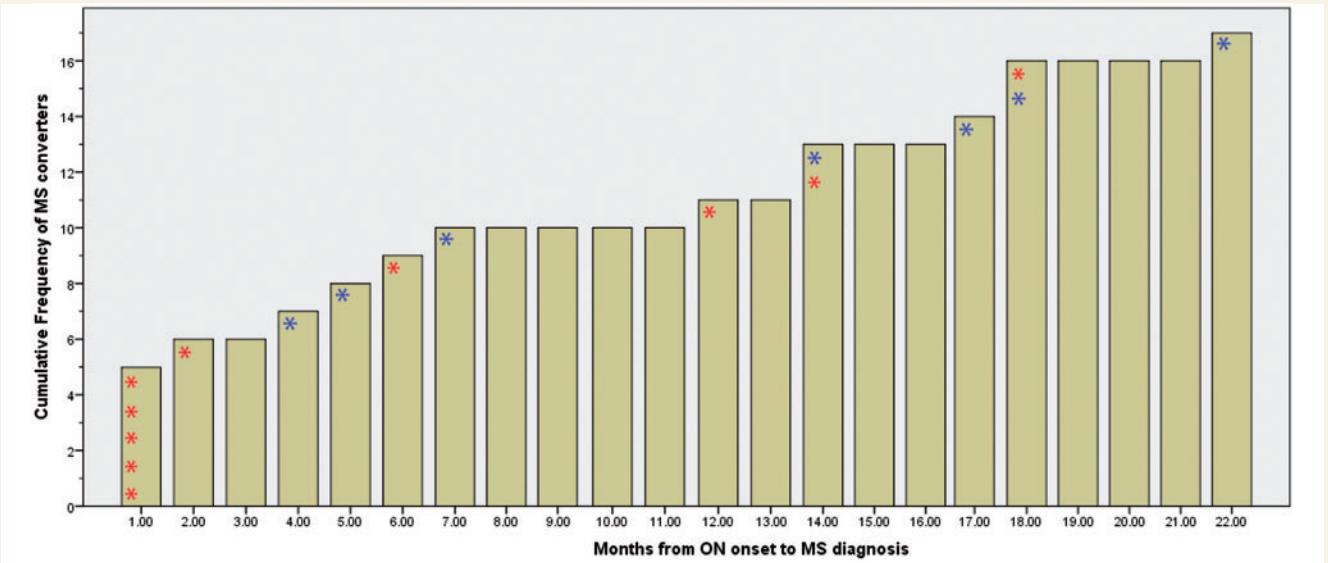

Figure 4 Cumulative incidence of conversion from optic neuritis to multiple sclerosis. The diagram shows the timing of multiple sclerosis (MS) diagnosis and initiation of first-line disease modifying treatment (interferon beta 1a). Note that all patients were untreated at optic neuritis (ON) onset, and decision for treatment initiation was made as either a preventative measure or after multiple sclerosis diagnosis. This decision was made by multiple sclerosis specialist doctors and was not influenced by the study. Red asterisk indicates that patient started on disease-modifying treatment at the same time as multiple sclerosis diagnosis. Blue asterisk indicates that patient started on preventative disease-modifying treatment 2–6 weeks after optic neuritis onset.

Table 2 Results of stepwise multivariate logistic regression with multiple sclerosis at 2 years as dependent variable

Variable	Values	Patients, *n*	MS conversion rate (%)	*P*-value	Odds ratio	95% CI
Number of white matter lesions	0–1	12	17	0.006[a]	–	
	2–8	13	31	0.42	3.7[b]	0.43–32.3
	⩾ 9	13	79	0.002	52.6[b]	3.3–233
Permeability in NAWM	–	–	–	0.03	8.5[c]	1.97–40.8
Oligoclonal bands	Yes	22	55	0.06	–	–
	No	12	25			
CSF leucocyte count	–	–	–	0.08	–	–
Age	–	–	–	0.18	–	–
Gender	Female	29	38	0.46	–	–
	Male	9	67			
CEL	Yes	4	100	0.99[d]	–	–
	No	34	38			

Number of white matter lesions and permeability in normal-appearing white matter provided the best model with a Nagelkerke $R^2 = 0.66$; $P = 0.00004$. Adding number of white matter lesions alone to the model provided a Nagelkerke $R^2 = 0.42$, but adding permeability in normal-appearing white matter significantly improved the model accuracy ($R^2 = 0.56$; $P = 0.007$), and adding oligoclonal bands provided ($R^2 = 0.66$; $P = 0.02$). Permeability in the thalamus was also a significant predictor of multiple sclerosis ($P = 0.035$), when entered instead of normal-appearing white matter permeability, but was left out to avoid problems of colinearity.

CEL = contrast enhancing lesions; NAWM = normal-appearing white matter; MS = multiple sclerosis.

[a]*P*-value for the categorical variable.

[b]Odds ratio when compared to the first group having 0–1 white matter lesions.

[c]Odds ratio for an increase in permeability of 0.1 ml/100 g/min.

[d]All contrast enhancing lesion positive patients had more than six lesions and permeability in normal-appearing white matter >0.13, thus contrast enhancing lesions did not provide additional risk information in this study.

some extent reflect the cellular permeability of the BBB. We have previously reported that patients with relapsing-remitting multiple sclerosis experiencing a relapse had higher permeability values in normal-appearing white matter and that immunomodulatory treatment attenuated this increase (Cramer *et al.*, 2014). Interestingly, the absolute level of permeability in untreated patients with relapsing-remitting multiple sclerosis was very similar to that of the optic neuritis patients who converted to multiple sclerosis in this study (K_i of 0.18 and 0.12 ml/100 g/min,

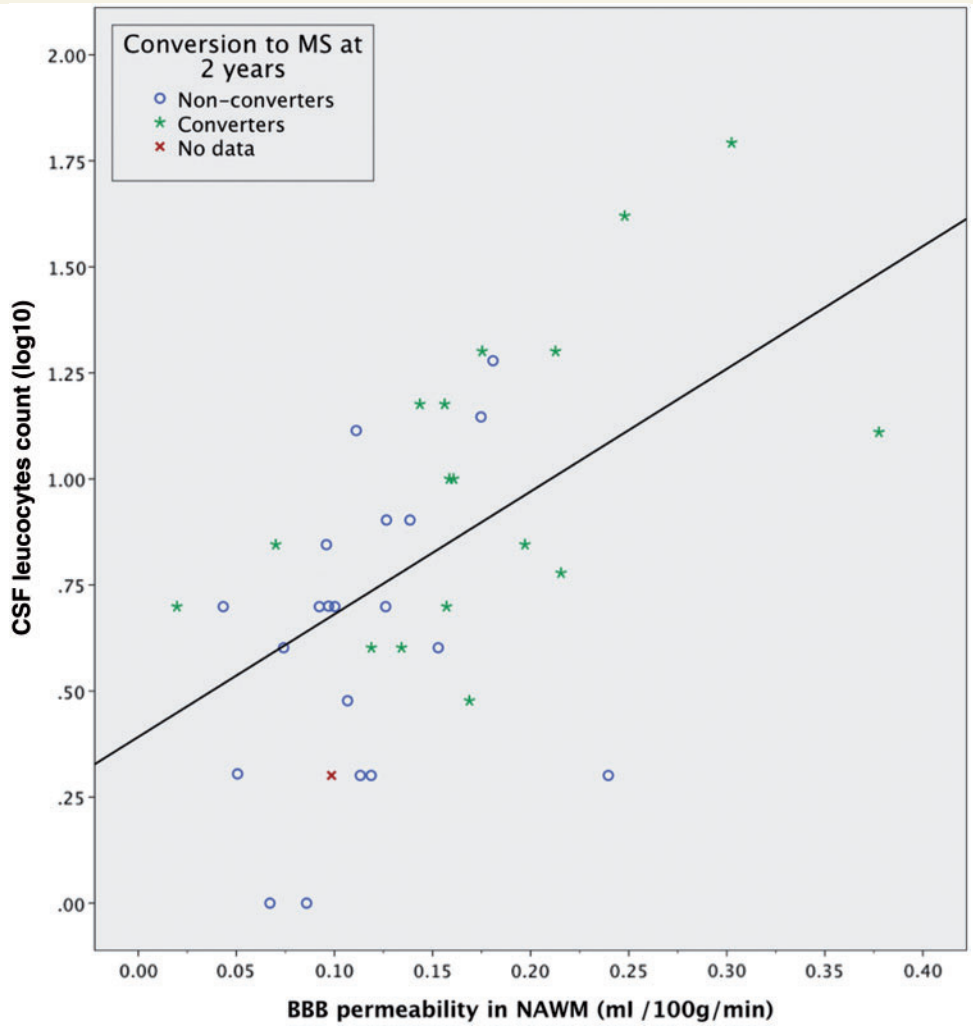

Figure 5 Permeability of the BBB in periventricular normal-appearing white matter plotted against CSF leucocyte count in optic neuritis patients. The blue circle and green star icons indicates multiple sclerosis conversion status for each patient after 2 years. Spearman CC 0.57; $P = 0.0002$. Linear fit line added for visualization purposes only. No data = no information on multiple sclerosis conversion status. NAWM = normal-appearing white matter.

respectively), arguing that widespread BBB opening in lesions as well as normal-appearing brain tissue might be linked directly to central pathophysiological mechanisms in multiple sclerosis. Taken together, these results indicate that permeability may provide a snapshot of the current level of multiple sclerosis-related neuroinflammation, whereas T_2 lesions may reflect the length of the subclinical pre-relapse phase.

We observe a conversion rate from optic neuritis to multiple sclerosis based on the 2010 McDonald criteria of 45% and to clinically definite multiple sclerosis of 16% at 2 years, which is slightly lower than reported elsewhere. D'Alessandro *et al.* (2013) reported conversion rates to McDonald multiple sclerosis after clinically isolated syndrome of 57% at 2 years; which is in line with previous reports of lower risk of conversion to multiple sclerosis after optic neuritis when compared to clinically isolated syndrome in general (Miller *et al.*, 2005). D'Alessandro *et al.* included a broad spectrum of patients with clinically isolated syndrome retrospectively with symptoms suggestive of multiple sclerosis from the past 6 months. Also, a slightly higher proportion of patients in our study were started on disease-modifying drugs 2–6 weeks after onset of optic neuritis (58%), compared to 49% in the study by D'Alessandro *et al.* (2013) who were started within the first year.

Six patients converted to multiple sclerosis shortly after baseline MRI, four due to positivity of the dissemination in time criteria (Fig. 4). In an attempt to evaluate if permeability would be of any use in a clinical setting, we excluded these six patients from the data set and found that permeability in normal-appearing white matter ($P = 0.027$) and CSF leucocyte count ($P = 0.023$) were now significant predictors of multiple sclerosis conversion with Nagelkerke $R^2 = 0.64$ and $P = 0.001$. Permeability in thalamus was also significant ($P = 0.019$) when added instead of normal-appearing white matter permeability. T_2 lesion count was no longer significant, presumably due to

Table 3 Results of receiver operating characteristic curve analysis

ROC analysis Specificity	AUC	*P*-value	Optimal cut-off	Sensitivity	
T_2 lesion count	0.86 (CI 0.73–0.98)	0.0001	>5	77%	82%
Permeability in NAWM	0.77 (CI 0.60–0.93)	0.005	0.13 ml/100 g/min	88%	71%
Permeability in the thalamus	0.78 (CI 0.63–0.93)	0.003	0.09 ml/100 g/min	82%	62%
CSF leucocytes	0.77 (CI 0.62–0.92)	0.005	>5 mio/l	71%	71%
Oligoclonal bands	0.67	0.069	–	82%	48%

AUC = area under the curve; NAWM = normal-appearing white matter; ROC = receiver operating characteristic.

Table 4 Relationship between permeability in normal-appearing white matter and investigated variables in patients with optic neuritis

CSF biomarkers	CC	*P*-value	*n*
IgG index	0.17	0.35	38[a]
Oligoclonal bands	n/a	0.72[c]	39
Leucocyte count (mio/l)	0.57	0.0002	38[a]
CXCL10 (pg/ml)	0.40	0.02	34
MMP9 (ng/ml)	n/a	0.034[b]	34
CXCL13 (pg/ml)	0.11	0.55	34
Albumin index (CSF/serum)	−0.02	0.91	38[a]
MRI variables			
T_2 lesion count	0.13	0.44	39
T_2 lesion load (mm^3)	0.25	0.19	39

[a]Due to high erythrocyte count in CSF we excluded IgG index, leucocyte count and albumin index for one patient.
[b]Censored regression (Tobit) analysis.
[c]Logistic regression analysis. CC = correlation coefficient.

exclusion of six subjects with high lesion count driving the significance. ROC curve analysis for permeability in normal-appearing white matter now showed an area under the curve of 0.81, $P = 0.005$ and a threshold of 0.13 ml/100 g/min gave a sensitivity of 91% and specificity of 71%. ROC curve analysis of CSF leucocyte count gave an area under the curve of 0.85; $P = 0.001$, and a threshold of 5 mio/l leucocytes gave a sensitivity of 82% and sensitivity of 71%. Four multiple sclerosis converters were not started on preventative disease-modifying treatment due to a low perceived multiple sclerosis risk (<3 white matter lesions; negative dissemination in space criteria; three had positive oligoclonal bands; three had CSF leucocytes >5mio/l). All four had permeability in normal-appearing white matter >0.13ml/100 g/min (Fig. 6). Thus, clinical access to a complementary biomarker of neuroinflammation might provide extra risk information in a subset of patients. Future prospects after optic neuritis are still very diverse, which merits further studying of potential biomarkers of multiple sclerosis conversion such as MRI permeability.

Permeability in normal-appearing white matter and in the thalamus

We found that permeability in both normal-appearing white matter and in the thalamus provide novel information on multiple sclerosis conversion, when compared to using T_2 lesions alone. This finding fits well with previous multiple sclerosis studies indicating early pathological changes in the thalamus such as atrophy, altered mean diffusivity, reduced *N*-acetyl-aspartate concentration and iron accumulation, whereas T_2 lesions are more pronounced in the later stages of the multiple sclerosis disease (Minagar *et al.*, 2013). However, we did not find a significant correlation between permeability in the thalamus and CSF biomarkers of leucocyte trafficking nor was thalamic permeability higher in the whole group of optic neuritis patients when compared to healthy controls. Although multiple sclerosis is increasingly being acknowledged as also being a grey matter disease, research has found that grey matter involvement differs significantly from white matter lesions. Features such as lymphocyte infiltration, complement deposition and BBB disruption are typically not detected in grey matter of autopsy samples and diffuse microglial activation is detectable in thalamic normal-appearing grey matter, but to a lesser extent than in the normal-appearing white matter (Vercellino *et al.*, 2009; Popescu and Lucchinetti, 2012). As the thalamus is comprised of a mixture of clusters of grey matter nuclei separated by medullary laminae of myelinated fibres, as well as larger tracts of white matter bundles, it seems plausible to assume that permeability as measured by DCE-MRI may primarily reflect the neuroinflammatory processes, which appears to be most prominent in the myelinated areas of the brain.

Limitations in study design

An important limitation in this study is the non-uniformity of which the follow-up procedure was performed. Optic neuritis patients who had many baseline white matter lesions were—for clinical reasons—investigated more intensively with MRI and clinical evaluation than those who had few white matter lesions, introducing a possible bias towards earlier diagnosis. On the other hand, those with many white matter lesions were frequently initiated in immunomodulatory treatment, presumably delaying conversion to multiple sclerosis. This bias may explain the heterogeneity in permeability values in the subset of optic neuritis patients who did not convert to multiple sclerosis. However, immunomodulatory treatment after the first relapse is now becoming the norm in patients with high

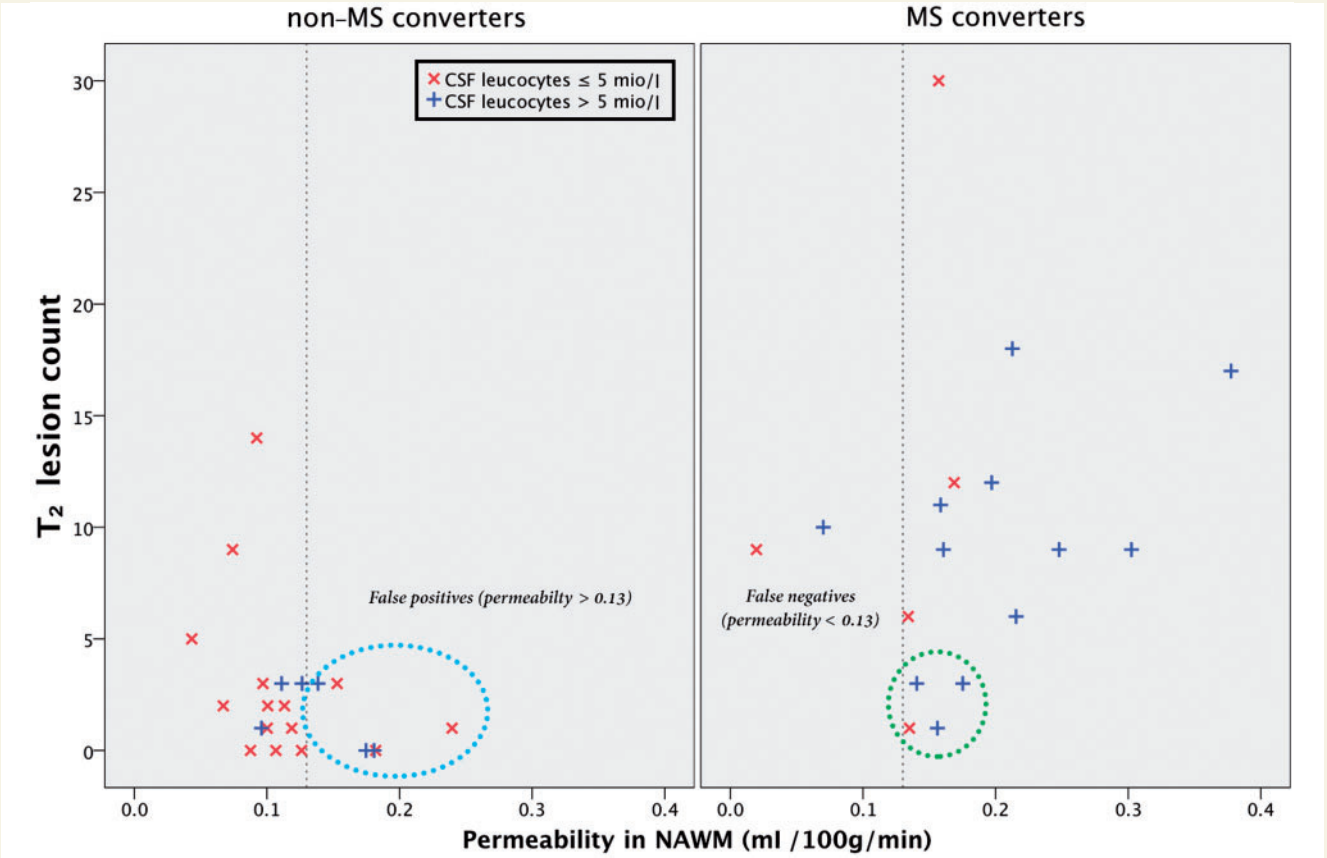

Figure 6 Performance of T_2 lesion count, permeability in normal-appearing white matter and CSF leucocytes to predict multiple sclerosis conversion. The vertical dotted line represents the normal-appearing white matter permeability threshold level of 0.13 ml/100 g/min found in the ROC analysis. Four patients (circled with green) were not started on disease-modifying treatment in part due to a low perceived future multiple sclerosis risk. However, all four had normal-appearing white matter permeability >0.13 ml/100 g/min and three had CSF leucocytes >5 mio/l. The blue circle highlights the six false positives that did not develop multiple sclerosis but had permeability >0.13 ml/100 g/min. NAWM = normal-appearing white matter.

multiple sclerosis risk, and any biomarker faces the challenge of having to perform within the frame of the actual everyday clinical set-up.

Methodological considerations

As the DCE-MRI method that we apply in this study attempts to measure very subtle differences in BBB permeability, we have previously published work testing the accuracy and precision of the method. We found that the method was able to significantly distinguish values as low as 0.1 ml/100 g/min from zero, provided that we use a long total measurement time of 15 min and a high time resolution of ~1 s (Cramer and Larsson, 2014). The conclusions of this study are thus based on a strong theoretical and methodological foundation. In this study, we chose to define regions of interest manually after careful consideration of the advantages and disadvantages compared to a more automated segmentation-based approach. Manual region of interest placement allows us to ensure similar size between all subjects and gives us better control of potential partial volume errors from CSF, vessels, grey matter and multiple sclerosis lesions. Every time a region of interest was placed, we looked through the corresponding three slices of a FLAIR T_2 with a slice thickness of 3.5 mm and same angulation as the 8 mm DCE slices. However, region of interest placement will still inevitably be different between subjects with high and low lesion loads. In an attempt to quantify this effect we conducted a test–retest reliability analysis that consisted of replacing the normal-appearing white matter regions of interest twice in the 15 subjects with two or fewer T_2 lesions, to a location more typical of a subject with high lesion load (Supplementary Fig. 4). Test–retest analysis gave a Crohnbach alpha of 0.94 and using the new values, did not change any of the results of the study. In addition, the lack of correlation between permeability on one side and lesion count and lesion load on the other, together with the fact that permeability in the thalamus also significantly predicted multiple sclerosis development, argues that our findings are not a result of region of interest positioning differences between subgroups with high and low lesion load.

BBB breach in optic neuritis and multiple sclerosis

The classic view of the CNS as a site of complete immunoprivilege has been challenged by the observation that activated T cells are readily able to penetrate the endothelial cell layer at the level of the post-capillary venules. Here they perform immune-surveillance in the perivascular and subarachnoid spaces without disturbing the barrier capabilities of the BBB (Britta Engelhardt, 2011). Solute diffusion across the BBB is—on the other hand—controlled at the capillary level, hence it is important to acknowledge that permeability of solutes and cells are not the same (Bechmann *et al.*, 2007). When activated T cells in the perivascular spaces encounter their specific antigen presenting cell they signal for opening of the endothelial cell layer through chemokines and interleukins, hereby mounting an immune response that attracts further immune cells to the site. The inner barrier, which is comprised of the glia limitans and its basement membrane, is then breached and an immune response mounted into the neuropil itself (Britta Engelhardt, 2011). Keeping this in mind, it remains challenging to conceive whether the subtle permeability increases we observe in normal-appearing white matter reflect trapping of contrast agent in the perivascular spaces or accumulation into the neuropil itself. The mechanisms for Gd-DTPA passage across the BBB is not known in detail, but increased passage of a large variety of macromolecules has been observed in the context of inflammation and enhanced cellular permeability in animal models of multiple sclerosis, and is generally considered to be the result of secondary opening of tight junctions, enhanced pinocytotic activity, or formation of transendothelial channels (Juhler *et al.*, 1985; Claudio *et al.*, 1989; de Vries *et al.*, 1997). T cell-derived cytokines may influence transport of various compounds into the brain and *in vitro* studies have shown that administration of TNF, IL1, and IL6 to monolayers of endothelial cells leads to an increase in the solute permeability (de Vries *et al.*, 1996). Thus, a very plausible mechanism for increased passage of Gd-DTPA across the BBB in the presence of inflammation, is that when activated T cells in the perivascular spaces encounter their specific antigen they elicit secondary widespread permeability changes of the BBB endothelial cell layer at both the post-capillary and capillary level resulting in increased 'bystander' passage of Gd-DTPA into the perivascular spaces. However, we also found a correlation between Gd-DTPA permeability and MMP9, which is required for degradation of laminin 1 and 2 of the glia limitans (Bechmann *et al.*, 2007; Britta Engelhardt, 2011). This indicates that Gd-DTPA-based measurements of BBB at least to some extent may reflect the cellular permeability into the neuropil itself. We found no correlation between permeability and CSF levels of albumin, measured as the albumin CSF/serum index, but all patients and healthy control subjects had values within normal range. This indicates that Gd-DTPA (547 Da), with a molecular weight more than 100 times smaller than albumin (66 437 Da), may be a more sensitive marker of low-grade BBB permeability changes.

Perspectives

In this study we found that permeability of the BBB in normal-appearing white matter, as measured by MRI, may provide novel pathological information on neuroinflammation in optic neuritis and multiple sclerosis, possibly providing a 'snapshot' of the present level of multiple sclerosis-related CNS inflammation. Currently, the most widely used measures of multiple sclerosis disease activity are occurrence of new MRI lesions and/or clinical relapses, but these measures do not always correlate well with long-term disability outcomes in clinical multiple sclerosis trials (Scalfari *et al.*, 2010) or annual atrophy rates in so-called benign multiple sclerosis (Gauthier *et al.*, 2009). This indicates the existence of ongoing subclinical disease activity even in the absence of relapses or MRI activity. Hence, a new marker of low-grade multiple sclerosis disease activity could have many useful applications, i.e. subclinical disease activity monitoring or identification of inadequate treatment response before the next relapse occurs. Furthermore, quantification of BBB permeability may constitute an early prognostic factor in the pathogenesis of multiple sclerosis, while MRI features such as multiple sclerosis plaques, loss of *N*-acetyl-aspartate, decrease of magnetic transfer ratio (MTR), changes in T_1, and tissue atrophy may be considered as consequences of a longer lasting neuroinflammation.

Acknowledgements

We would like to thank radiographers Bente Sonne Møller and Karina Elin Segers at Dept. of Radiology, Rigshospitalet, Glostrup. Ulrich Lindberg for Matlab help. We would like to express our gratitude to the patients for participating.

Funding

This work was supported by The Research Foundation of the Capital Region of Denmark, Foundation for Health Research [grant number R129-A4197]; Biogen Idec [grant number GLO-01-2012]; and The Danish Multiple Sclerosis Society [grant number 14588].

Supplementary material

Supplementary material is available at *Brain* online.

References

Avolio C, Ruggieri M, Giuliani F, Liuzzi GM, Leante R, Riccio P, et al. Serum MMP-2 and MMP-9 are elevated in different multiple sclerosis subtypes. J Neuroimmunol 2003; 136: 46–53.

Barkhof F, Miller D, Scheltens P, Campi A, Polman C, Filippi M. Comparison of MRI criteria at first presentation to predict conversion to clinically definite multiple sclerosis. Brain 1997; 120: 2059–69.

Bechmann I, Galea I, Perry VH. What is the blood-brain barrier (not)? Trends Immunol 2007; 28: 5–11.

Britta Engelhardt CC. Fluids and barriers of the CNS establish immune privilege by confining immune surveillance to a two-walled castle moat surrounding the CNS castle. Fluids Barriers CNS 2011; 8: 4.

Claudio L, Kress Y, Norton WT, Brosnan CF. Increased vesicular transport and decreased mitochondrial content in blood-brain barrier endothelial cells during experimental autoimmune encephalomyelitis. Am J Pathol 1989; 135: 1157.

Clerico M, Faggiano F, Palace J, Rice G, Tintorè M, Durelli L. Recombinant interferon beta or glatiramer acetate for delaying conversion of the first demyelinating event to multiple sclerosis. [Internet]. Cochrane Database Syst Rev 2008: CD005278.[cited 2015 Mar 30] http://www.ncbi.nlm.nih.gov/pubmed/18425915

Cramer SP, Simonsen H, Frederiksen JL, Rostrup E, Larsson HBW. Abnormal blood–brain barrier permeability in normal appearing white matter in multiple sclerosis investigated by MRI. Neuroimage: Clinical 2014; 4: 182–9.

Cramer SP, Larsson HBW. Accurate determination of blood-brain barrier permeability using dynamic contrast-enhanced T1-weighted MRI: a simulation and in vivo study on healthy subjects and multiple sclerosis patients. J Cereb Blood Flow Metab 2014: 1–11. http://www.ncbi.nlm.nih.gov/pubmed/25074746

de Vries HE, Blom-Roosemalen MC, van Oosten M, de Boer AG, Van Berkel TJ, Breimer DD, et al. The influence of cytokines on the integrity of the blood-brain barrier *in vitro*. J Neuroimmunol 1996; 64: 37–43.

de Vries HE, Kuiper J, de Boer AG, Van Berkel TJ, Breimer DD. The blood-brain barrier in neuroinflammatory diseases. Pharmacol Rev 1997; 49: 143–55.

D'Alessandro R, Vignatelli L, Lugaresi A, Baldin E, Granella F, Tola MR, et al. Risk of multiple sclerosis following clinically isolated syndrome: a 4-year prospective study. J Neurol 2013; 260: 1583–93.

Gauthier SA, Berger AM, Liptak Z, Duan Y, Egorova S, Buckle GJ, et al. Rate of brain atrophy in benign vs early multiple sclerosis. Arch Neurol 2009; 66: 234–37.

Gout O, Bouchareine A, Moulignier A, Deschamps R, Papeix C, Gorochov G, et al. Prognostic value of cerebrospinal fluid analysis at the time of a first demyelinating event. Mult Scler 2011; 17: 164–72.

Hansen AE, Pedersen H, Rostrup E, Larsson HBW. Partial volume effect (PVE) on the arterial input function (AIF) in T1-weighted perfusion imaging and limitations of the multiplicative rescaling approach. Magn Reson Med 2009; 62: 1055–9.

Juhler M, Blasberg RG, Fenstermacher JD, Patlak CS, Paulson OB. A spatial analysis of the blood-brain barrier damage in experimental allergic encephalomyelitis. J Cereb Blood Flow Metab 1985; 5: 545–53.

Khademi M, Kockum I, Andersson ML, Iacobaeus E, Brundin L, Sellebjerg F, et al. Cerebrospinal fluid CXCL13 in multiple sclerosis: a suggestive prognostic marker for the disease course. Mult Scler 2011; 17: 335–43.

Larsson HBW, Courivaud F, Rostrup E, Hansen AE. Measurement of brain perfusion, blood volume, and blood-brain barrier permeability, using dynamic contrast-enhanced T1-weighted MRI at 3 tesla. Magn Reson Med 2009; 62: 1270–81.

Larsson HBW, Hansen AE, Berg HK, Rostrup E, Haraldseth O. Dynamic contrast-enhanced quantitative perfusion measurement of the brain usingT1-weighted MRI at 3T. J. Magn Reson Imaging 2008; 27: 754–62.

Leppert D. Matrix metalloproteinase-9 (gelatinase B) is selectively elevated in CSF during relapses and stable phases of multiple sclerosis. Brain 1998; 121: 2327–34.

Minagar A, Barnett MH, Benedict RHB, Pelletier D, Pirko I, Sahraian MA, et al. The thalamus and multiple sclerosis: Modern views on pathologic, imaging, and clinical aspects. Neurology 2013; 80: 210–19.

Miller D, Barkhof F, Montalban X, Thompson A, Filippi M. Clinically isolated syndromes suggestive of multiple sclerosis, part I: Natural history, pathogenesis, diagnosis, and prognosis. Lancet Neurol 2005; 4: 281–288.

Modvig S, Degn M, Horwitz H, Cramer SP, Larsson HBW, Wanscher B, et al. Relationship between cerebrospinal fluid biomarkers for inflammation, demyelination and neurodegeneration in acute optic neuritis. PLoS One 2013; 8: e77163.

Modvig S, Degn M, Roed H, Sorensen T, Larsson H, Langkilde A, et al. Cerebrospinal fluid levels of chitinase 3-like 1 and neurofilament light chain predict multiple sclerosis development and disability after optic neuritis. Mult Scler J 2015: 1–10. [Epub ahead of print].

Optic Neuritis Study Group. Multiple sclerosis risk after optic neuritis: final optic neuritis treatment trial follow-up. Arch Neurol 2008; 65: 727–32.

Polman CH, Reingold SC, Banwell B, Clanet M, Cohen JA, Filippi M, et al. Diagnostic criteria for multiple sclerosis: 2010 revisions to the McDonald criteria. Ann Neurol 2011; 69: 292–302.

Popescu BF, Lucchinetti CF. Meningeal and cortical grey matter pathology in multiple sclerosis. BMC Neurol 2012; 12: 11.

Scalfari A, Neuhaus A, Degenhardt A, Rice GP, Muraro PA, Daumer M, et al. The natural history of multiple sclerosis, a geographically based study 10: relapses and long-term disability. Brain 2010; 133: 1914–29.

Sellebjerg F, Sorensen TL. Chemokines and matrix metalloproteinase-9 in leukocyte recruitment to the central nervous system. Brain Res Bull 2003; 61: 347–55.

Sorensen TL, Sellebjerg F, Jensen CV, Strieter RM, Ransohoff RM. Chemokines CXCL10 and CCL2: differential involvement in intrathecal inflammation in multiple sclerosis. Eur J Neurol 2001; 8: 665–72.

Tintoré M, Rovira A, Martínez MJ, Rio J, Díaz-Villoslada P, Brieva L, et al. Isolated demyelinating syndromes: Comparison of different MR imaging criteria to predict conversion to clinically definite multiple sclerosis. Am J Neuroradiol 2000; 21: 702–6.

Vercellino M, Masera S, Lorenzatti M, Condello C, Merola A, Mattioda A, et al. Demyelination, inflammation, and neurodegeneration in multiple sclerosis deep gray matter. J Neuropathol Exp Neurol 2009; 68: 489–502.

van Osch MJ, Vonken EJ, Bakker CJ, Viergever MA. Correcting partial volume artifacts of the arterial input function in quantitative cerebral perfusion MRI. Magn Reson Med 2001; 45: 477–85.